Contribution from the Department of Chemistry,
Columbia University, New York, New York 10027

Synthesis and Characterization of Physical, Electronic, and Photochemical Aspects of 9,10-Phenanthrenequinone Diimine Complexes of Ruthenium(II) and Rhodium(III)

Anna Marie Pyle,† Michael Y. Chiang,‡ and Jacqueline K. Barton*,§

Received February 23, 1990

A series of ruthenium(II) and rhodium(III) complexes containing the novel 9,10-phenanthrenequinone diimine (phi) ligand have been prepared and characterized with respect to structure, spectroscopy, and/or photochemical reactivity. Synthetic approaches to mixed-ligand complexes containing the phi ligand include direct addition of the protected *N,N'*-bis(trimethylsilyl)-phenanthrenequinone diimine ligand to the metal center or chelation first of diaminophenanthrene followed by oxidation to the coordinated phi ligand. With these strategies, $Rh(phen)_2(phi)^{3+}$, $Rh(phi)_2(bpy)^{3+}$, and $Rh(phi)_3^{3+}$ as well as their ruthenium(II) counterparts have been prepared. A crystal structure of $[Ru(bpy)_2(phi)](BF_4)_2 \cdot 0.19H_2O$ is reported (monoclinic crystal system, space group $P2_1/n$, $Z = 4$; $a = 9.56$ (9) Å, $b = 15.98$ (2) Å, $c = 21.24$ (2) Å, $\beta = 93.61$ (7)°, $V = 3238$ (5) Å^3) and indicates substantial back-bonding to the metal center of the phi ligand in comparison to the polypyridyls and a novel shape of the complex as a result of the jutting out of the flat, expansive phi ligand from the metal. The series of mixed-ligand complexes of ruthenium(II) containing phi and bpy exhibit novel charge-transfer transitions at progressively lower energies with increasing phi substitution, suggesting the possibility of a unique delocalized excited state with phi ligands coordinated. Electronic spectra for the rhodium(III) series are found to be quite similar to their rhodium(III) polypyridyl analogues, being dominated by ligand transitions, although for the phi complexes, variations with pH are observed (pK_a of $Rh(phen)_2phi^{3+} = 6.1 \pm 0.1$; pK_1 and pK_2 of $Rh(phi)_2(bpy)^{3+} = 6.8 \pm 0.2$). Also as with their polypyridyl counterparts, phi complexes of rhodium(III) undergo photodecomposition, with the preferential loss of the phi ligand in mixed-ligand complexes ($\Phi_{313} = 0.0027$ and 0.000 21 for $Rh(phen)_2phi^{3+}$ and $Rh(phi)_2bpy^{3+}$, respectively). Owing to their unique shapes and electronic characteristics, phi complexes represent promising reagents in developing probes for nucleic acid structure.

Introduction

Over the past several years there has been rapid development of a new class of coordination complexes containing the 9.10-phenanthrenequinone diimine (phi) ligand.[1-6] As many coordination complexes of ruthenium(II) and rhodium(III) have become important tools in the fields of energy research[7] and biological chemistry,[8] new ligand systems have been sought in order to further tune and modulate the properties of this particularly useful family of d^6 coordination complexes. The phi ligand, for example, has properties significantly different from those of the well-studied polypyridyl ligand system, and it is becoming clear that these unusual properties will allow unique applications of ruthenium and rhodium complexes containing the phi ligand.

In our laboratory, phi complexes are being exploited as sensitive probes of nucleic acid structure. Both ruthenium(II) and rhodium(III) complexes containing the phi ligand have been found to bind DNA avidly by intercalation between base pairs.[5,6] Mixed-ligand complexes of ruthenium(II) containing phi have been useful in spectroscopic experiments to explore the factors that govern intercalative binding to DNA.[5] Rhodium(III) complexes containing phi have found a particularly wide range of application as photoactivated probes of local DNA helical conformation[6,9] and RNA tertiary structure[10] and as high-resolution DNA footprinting reagents.[11] Despite the ever increasing applications of these complexes, however, there has been little discussion of their physical and photochemical properties. In this report we describe the coordination chemistry of phi complexes of ruthenium and rhodium and we illustrate some unusual properties intrinsic to this new class of molecules.

Experimental Section

Syntheses of Metal Complexes. $[Rh(phen)_2Cl_2]Cl$. This complex was prepared as described in the literature[12] but with some modification. The reaction is vigorously refluxed at 100 °C rather than 60 °C in order to facilitate complete reaction within 2 h. NMR (D_2O): 9.51 (1, d), 9.02 (1, d), 8.63 (1, d), 8.34 (1, t), 8.29 (1, d), 8.15 (1, d), 7.70 (1, d), 7.48 ppm (1, t).

$[Rh(phen)_2(H_2O)_2](NO_3)_3$. Freshly prepared Ag_2O (5.9 mmol) is washed thoroughly with H_2O and added as a wet slurry to a 10-mL aqueous solution of $[Rh(phen)_2Cl_2]Cl$ (0.55 mmol), and the slurry is stirred in the dark for 24 h at 25 °C. After the reaction mixture is filtered, the filtrate is acidified to pH 1 with HNO_3. Acidification yields a colorless solution from which, when reduced to 2 mL in volume, precipitates pale yellow $[Rh(phen)_2(H_2O)_2](NO_3)_3$ crystals. After collection on a frit, the crystals are washed with cold ethanol. This preparation is adapted from the synthesis of an analogous Co(III) complex.[13] NMR (D_2O): 9.80 (1, d), 8.92 (1, d), 8.50 (1, d), 8.21 (1, t), 8.19 (1, d), 8.05 (1, d), 7.64 (1, d), 7.40 ppm (1, dd). FABMS ion mass (m/e): 463, $Rh(phen)_2^+$; 480, $Rh(phen)_2(OH)^+$; 497, $Rh(phen)_2(OH)_2^+$.

$[Rh(phen)_2(phi)]Cl_3$. After $[Rh(phen)_2(H_2O)_2](NO_3)_3$ crystals (0.18 mmol) are dissolved in 3 mL of H_2O, diaminophenanthrene (0.22 mmol) suspended in 5 mL of EtOH is added dropwise to the solution. Both solutions must be individually purged of O_2 and transferred against a flow of N_2. The mixture is refluxed under N_2 for 24 h, and the resultant orange-brown solution is then stirred at 25 °C in air for 24 h. KCl is added to the solution and the volume reduced. $[Rh(phen)_2(phi)]Cl_3$ is precipitated from methanol/acetone. $[Rh(phen)_2(phi)](PF_6)_3$ is precipitated by adding a saturated aqueous solution of KPF_6 to an ethanolic solution of $[Rh(phen)_2(phi)]Cl_3$ and washing the precipitate thoroughly with H_2O. NMR of $[Rh(phen)_2(phi)]Cl_3$ (DMSO): 14.98 (2, s, N–H), 9.25 (2, d), 9.12 (2, d), 9.03 (2, d), 8.94 (2, d), 8.54 (4, dd), 8.47 (2, d), 8.36 (2, dd), 8.08 (2, d), 7.91 (2, dd), 7.84 (2, t), 7.57 ppm (2, t). NMR (D_2O): 8.932 (1, d, 8.36 Hz), 8.846 (1, t, 5.28), 8.731 (1, t, 8.36), 8.226 (2, q, 6.48), 8.123 (1, d, 8.32), 8.026 (2, m), 7.812 (1, d, 5.28), 7.660 (1,

* To whom correspondence should be addressed.
† Present address: Department of Chemistry and Biochemistry, University of Colorado, Boulder, CO 80309.
‡ Present address: Department of Chemistry, Washington University, St. Louis, MO 63130.
§ Present address: Division of Chemistry and Chemical Engineering, California Institute of Technology, Pasadena, CA 91125.

(1) Belser, P.; von Zelewsky, A.; Zehnder, M. *Inorg. Chem.* **1981**, *20*, 3098.
(2) Juris, A.; Barigelletti, F.; Balzani, V.; Belser, P.; von Zelewsky, A. *Isr. J. Chem.* **1982**, *22*, 87. Dapporto, P.; Denti, G.; Dolcetti, G.; Ghedini, M. *J. Chem. Soc., Dalton Trans.* **1983**, 779. Rehorek, D.; Thomas, P. *Z. Chem.* **1977**, *17*, 112.
(3) Schlosser, K.; Hoyer, E. *Z. Chem.* **1970**, *10*, 439–440. Schlosser, K.; Hoyer, E. *J. Inorg. Nucl. Chem.* **1971**, *33*, 4370–4371.
(4) Pyle, A. M.; Barton, J. K. *Inorg. Chem.* **1986**, *26*, 3820–3823.
(5) Pyle, A. M.; Rehmann, J. P.; Meshoyrer, R.; Kumar, C. V.; Turro, N. J.; Barton, J. K. *J. Am. Chem. Soc.* **1989**, *111*, 3051.
(6) Pyle, A. M.; Long, E. C.; Barton, J. K. *J. Am. Chem. Soc.* **1989**, *111*, 4520.
(7) Juris, A.; Balzani, V.; Barigelletti, F.; Campagna, S.; Belser, P.; Von Zelewsky, A. *Coord. Chem. Rev.* **1988**, *84*, 85. Meyer, T. J. *Pure Appl. Chem.* **1986**, *58*, 1193. Seddon, K. R. *Coord. Chem. Rev.* **1985**, *67*, 171. Sutin, N.; Creutz, C. *Pure Appl. Chem.* **1980**, *52*, 2717.
(8) Barton, J. K. *Science* **1986**, *233*, 727. Fleisher, M. B.; Mei, H.-Y.; Barton, J. K. *Nucleic Acids Mol. Biol.* **1988**, *2*, 65. Pyle, A. M.; Barton, J. K. *Prog. Inorg. Chem.*, in press.
(9) Pyle, A. M.; Morii, T.; Barton, J. K. Submitted for publication.
(10) Chow, C. S.; Barton, J. K. *J. Am. Chem. Soc.* **1990**, *112*, 2839.
(11) Uchida, K.; Pyle, A. M.; Morii, T.; Barton, J. K. *Nucl. Acids Res.* **1989**, *17*, 10259.
(12) Gillard, R. D.; Osborn, J. A.; Wilkinson, G. *J. Chem. Soc.* **1965**, 1951–1965.
(13) Ablov, A. V. *Russ. J. Inorg. Chem.* (*Engl. Transl.*) **1961**, *6*, 157–161.

0020-1669/90/1329-4487$02.50/0

t, 7.24), 7.624 (1, dd, 5.52), 7.355 ppm (1, t, 7.56 Hz). FABMS ion mass (m/e): 668, $Rh(phen)_2(phi)^+$; 489, $Rh(phen)(phi)^+$; 463, $Rh(phen)_2^+$. Anal. Calcd (found) for $[Rh(phen)_2(phi)](PF_6)_3 \cdot C_2H_5OH$: C, 41.76 (42.38); H, 2.80 (2.62); N, 7.30 (7.67).

$[Rh(phi)_2Cl_2]Cl$. $RhCl_3$ (Aesar 42.5% Rh, 0.41 mmol) is dissolved for 20 min in 5 mL of anhydrous EtOH with gentle heating. Diaminophenanthrene (DAP, 0.9 mmol) and solid $N_2H_4 \cdot HCl$ (0.05 mmol) are placed in a dry side-arm flask and stirred together with 15 mL of DMF. Both solutions are then purged separately with nitrogen for 20 min. Fresh, reagent grade solvents are used, and solids are dried thoroughly before use. After the systems are purged with N_2, the ethanolic $RhCl_3$ solution is added dropwise to the DAP/DMF slurry, against a flow of nitrogen. At first, the reaction turns an olive green color and then yellow. The reaction mixture is heated at 80 °C for 7 h or until the solution and solid floating in solution are yellow in color. The suspension is then opened to air and stirred in an open beaker, away from the light for 24–36 h at 25 °C or until both solution and solid precipitate are bright orange in color. Upon initial exposure to air, the solution becomes olive green again but then slowly turns bright orange. After this air-oxidation step, bright orange $[Rh(phi)_2Cl_2]Cl$ solid is filtered from solution. The complex is soluble only in DMF and DMSO. NMR spectroscopy of the product reveals that both cis and trans isomers are formed. However, they are both able to react with a third bidentate ligand to produce trischelated product, so no attempts were made to separate them routinely. The trans isomer is more soluble than the cis isomer as identified by NMR spectroscopy. Yield: 50–75%. NMR (DMSO), trans product: 14.89 (1, s, N–H), 8.75 (1, d), 8.53 (1, d), 7.92 (1, t), 7.82 ppm (1, t). (DMSO), cis product: 14.53 (1, s, N–H), 13.19 (1, s, N–H), 9.23 (1, d), 8.5 (2, t), 8.37 (1, d), 7.95 (1, d), 7.8 (1, d), 7.75 (1, t), 7.58 ppm (1, t). FABMS ion mass (m/e): 585, 587, $Rh(phi)_2Cl_2^+$; 549, $Rh(phi)_2Cl^+$; 515, $Rh(phi)_2^+$. Anal. Calcd (found) for $[Rh(phi)_2Cl_2]Cl$: C, 54.00 (55.24); H, 3.23 (3.52); N, 9.00 (8.79).

$[Rh(phi)_3]Cl_3$. This synthesis is a modification of a literature preparation.[14a] *N,N'*-Bis(trimethylsilyl)phenanthrenequinone diimine[14b] (0.153 mmol) is dissolved under N_2 in dry benzene (20 mL). This solution is syringed dropwise into a solution of $RhCl_3 \cdot 3H_2O$ (0.038 mmol) in 20 mL of dry, degassed EtOH while being stirred vigorously under N_2. The solution is stirred at room temperature in the absence of air and light for 24 h. The reaction mixture is then filtered to yield solid $[Rh(phi)_3]Cl_3$. NMR (DMSO): 14.42 (1, s, N–H), 8.68 (1, d), 8.53 (1, d), 7.93 (1, t), 7.81 ppm (1, t). FABMS ion mass (m/e): 720, $Rh(phi)_3^+$; 585, $Rh(phi)_2Cl_2^+$; 550, $Rh(phi)_2Cl^+$; 515, $Rh(phi)_2^+$.

$[Rh(phi)_2(bpy)]Cl_3$. $[Rh(phi)_2Cl_2]Cl$ (0.08 mmol) is quantitatively converted to the water-soluble $[Rh(phi)_2(bpy)]Cl_3$ by heating with polypyridyl (2,2'-bipyridyl, 0.1 mmol) and 0.1 equiv of $N_2H_4 \cdot HCl$ (0.011 mmol) in 3:1 DMF/H_2O. $[Rh(phi)_2Cl_2]Cl$ and bipyridyl are first partially dissolved in DMSO (30 mL) with gentle heating. Then, 10 mL of H_2O, containing the $N_2H_4 \cdot HCl$, is added dropwise to the warm DMF solution. The resulting suspension is heated at 100 °C in the presence of air. After 8 h, the suspension clarifies and becomes more orange in color. The reaction is then cooled to room temperature and any remaining solids are filtered out. The clear orange filtrate is stripped of solvent by vacuum, and the highly soluble product is taken up in H_2O. The aqueous solution is filtered again and extracted with $CHCl_3$ and diethyl ether, respectively, until the orange phase is colorless. Crystalline product is then isolated from the aqueous layer upon addition of KCl (25 mg) and reduction of volume. NMR (DMSO): 14.13 (2, s, N–H), 13.63 (2, s, N–H), 8.92 (2, d), 8.66 (6, m), 8.45 (6, d), 7.84 (6, m), 7.61 ppm (4, t). NMR (D_2O): 8.515 (1, d, 7.92), 8.331 (1, d, 5.88), 8.243 (1, t, 7.96), 8.181 (1, d, 8.0), 8.150 (1, d, 5.56), 8.130 (1, d, 5.44), 8.067 (1, d, 8.04), 7.690 (1, t, 8.04), 7.658 (1, t, 7.52), 7.610 (1, t, 7.16), 7.429 (1, t, 8.28), 7.391 ppm (1, t, 7.52 Hz). FABMS ion mass (m/e): 671, $Rh(phi)_2(bpy)^+$; 515, $Rh(phi)_2^+$; 465, $Rh(phi)(bpy)^+$. Anal. Calcd (found) for $[Rh(phi)_2(bpy)](PF_6)_3$: C, 41.25 (41.1); H, 2.55 (2.50); N, 7.60 (7.11).

Phi Complexes of Ruthenium(II). The synthesis and characterization of $[Ru(phi)_3]Cl_2$, $[Ru(bpy)_2(phi)]Cl_2$, $[Ru(phen)_2(phi)]Cl_2$, and $[Ru(phi)_2(bpy)]Cl_2$ have been described previously.[1,4,5]

Methods. Spectral Techniques. ^1H NMR spectra were recorded on Varian VXR-200, VXR-300, and VXR-400 spectrometers. Fast atom bombardment mass spectra, elemental analyses, fluorescence spectra, UV–visible spectra, and extinction coefficients were obtained as described previously.[4-6] Xe atoms were used for bombardment by FAB mass spectrometry. Ion peaks observed by using this method are properly reported as M^+ peaks, where M represents the molecular weight of a given fragment. Multivalent ions (and metal complexes in particular) are reduced to +1 species while undergoing analysis by FABMS, so ion masses are reported as +1 species in spite of the fact that the complexes under study may be +2 and +3 ions.[15] In addition, the Rh(III) complexes have a tendency to be one molecular weight unit smaller than the calculated molecular weight of the ion. This is probably due to the fact that phi coordinated to Rh(III) is known to be acidic (vida infra) and proton loss within the FABMS probe leads to a reduction in apparent molecular weight.

Table I. Crystallographic Data for $[(C_{34}H_{36}N_6Ru)(BF_4)_2] \cdot 0.19H_2O$

Crystal Data	
empirical formula	$[(C_{34}H_{36}N_6Ru)(BF_4)_2] \cdot 0.19H_2O$
color, habit	black prism
cryst size, mm	0.30 × 0.35 × 0.80
space group	$P2_1/n$
cryst system	monoclinic
unit cell dimens	
a, Å	9.560 (9)
b, Å	15.982 (15)
c, Å	21.237 (17)
α, deg	90.0
β, deg	93.61 (7)
γ, deg	90.0
V, Å^3	3238 (5)
Z	4
fw	806.8
ρ_{calcd}, g cm^{-3}	1.65
abs coeff μ, cm^{-1}	5.70
$F(000)$	1639.5
Data Collection	
diffractometer	Nicolet R3m
radiation	Mo Kα (λ = 0.71073 Å)
T, °C	25
monochromator	highly oriented graphite crystal
2θ range, deg	3.5–44.0
scan type	2θ–θ
index ranges	$-h, -k, \pm l$
no. of reflcns collcd	4352
no. of independ reflcns	3896
no. of obsd reflcns	3247 ($F > 6.0\sigma(F)$)
abs cor	empirical
Solution and Refinement	
syst	Siemens SHELXTL (Data General NOVA 4)
soln	direct methods
refinement method	full-matrix least squares
quant minimized	$\sum w(F_o - F_c)^2$
weighting scheme	$w = [\sigma^2(F_o) + 0.0039(F_o)^2]^{-1}$
$R(F_o)^a$	0.0288
$R_w(F_o)^b$	0.0308
largest Δ/σ	0.14
data:param ratio	8.3:1
largest difference peak, e/Å^3	0.25

$^a R(F_o) = \sum||F_o| - |F_c||/\sum|F_o|$. $^b R_w(F_o) = (\sum w||F_o| - |F_c||^2/\sum|F_o|^2)^{1/2}$.

For measurements of electronic spectra, because the spectra of the rhodium complexes were found to be pH-sensitive (vida infra), extinction coefficients of the rhodium complexes were measured in 50 mM tris and 20 mM sodium acetate, pH 7, by using the well-characterized $Rh(phen)_3^{3+}$ as an internal standard.[16] Concentrations of the complexes in solution were routinely measured optically at pH-independent isosbestic points: for $Rh(phen)_2(phi)^{3+}$ at 362 nm (19 400 M^{-1} cm^{-1}) and for $Rh(phi)_2(bpy)^{3+}$ at 350 nm (23 600 M^{-1} cm^{-1}). pH titrations were performed with an Orion Model SA720 pH meter. Studies of photodecomposition were performed by using a Model 6140 Oriel 1000-W Hg/Xe lamp with monochromator as a light source. Quartz cuvettes used in the irradiations were unmasked 1 cm × 1 cm × 3 cm cells fitted with Teflon plugs and stir bars.

Crystallographic Studies of $[Ru(bpy)_2(phi)](BF_4)_2 \cdot 0.19H_2O$. Black prismatic crystals of the complex $[Ru(bpy)_2(phi)](BF_4)_2 \cdot 0.19H_2O$ were obtained after recrystallization from ethanol, and a single crystal (0.30

(14) (a) Schlosser, K.; Hoyer, E. *Z. Anorg. Allg. Chem.* **1972**, *387*, 91–106. (b) Tuchtenhagen, G.; Ruhlmann, K. *Justus Liebigs Ann. Chem.* **1968**, *711*, 174.

(15) An electron-rich plasma on the surface of the probe is known to reduce metal complexes and organic molecules to lower oxidation states, giving rise to ions detected primarily as M^+ species: Cerny, R. L.; Sullivan, B. P.; Bursey, M. M.; Meyer, T. J. *Anal. Chem.* **1983**, *55*, 1954.

(16) McKenzie, E. D.; Plowman, R. A. *J. Inorg. Nucl. Chem.* **1970**, *32*, 199.

× 0.35 × 0.80 mm) was selected, mounted on a glass fiber, and subjected to an X-ray diffraction study. Crystal data are given in Table I.

Data were collected on an automated Nicolet R3m diffractometer at ambient temperature with a θ–2θ scan mode using graphite-monochromated Mo Kα radiation. All data collection and calculations were carried out on a NOVA4 computer with the SHELXTL crystallographic program package. A total of 4352 reflections ($-h,-k,\pm l$) were collected over the range $3.5° \leq 2\theta \leq 44°$. A total of 3896 unique reflections of 4352 measured reflections were considered, and 3247 reflections with $I > 3\sigma(I)$ were used in the following calculations. An empirical absorption correction based on azimuthal scans was applied.

The structure was solved by direct methods and refined by the full-matrix least-squares method, minimizing $\sum w(\Delta F)^2$. All non-H atoms (except water O_w) were refined anisotropically. The positions of the imine hydrogen atoms were located and refined. All other hydrogen atoms were calculated (assuming $d_{C-H} = 0.96$ Å) and put in as a riding model in the least-squares calculation. The final R value was 0.0288 and $R_w = 0.0308$ with $w = [\sigma^2(F_o) + 0.0039(F_o)^2]^{-1}$. The largest peak in the final difference electron density map was 0.25 e/Å^3.

Electronic Spectrum of Phi Ligand. The UV–visible spectrum of the phi ligand was obtained by dissolving the protected bis(trimethylsilyl)-phenanthrenequinone diimine (phi(TMS)$_2$) in dry heptane under nitrogen and transferring the solution to a sealed cuvette. After the phi(TMS)$_2$ solution was scanned $^1/_{100}$ volume of dry ethanol was added to the cuvette and the solution was scanned after 5 min of standing at room temperature. A blue shift could be observed as the ligand was desilylated and protonated. Under nitrogen in the cuvette, no apparent decomposition of the phi ligand could be observed (as measured spectroscopically). As solid phi ligand proved too unstable for isolation, extinction coefficients were not determined.

Measurement of pH-Dependent Optical Changes. A 20-mL solution of Rh(phen)$_2$(phi)$^{3+}$ or Rh(phi)$_2$(bpy)$^{3+}$ (20–30 μM) in pH 4.5 tris–acetate buffer was stirred vigorously while being monitored with a pH meter. After addition of 20–160-μL aliquots of 1 N NaOH to the solutions, the pH was recorded and 1 mL of solution was withdrawn for recording the UV–vis spectrum. After scanning, the solution was returned to the remaining 19 mL of solution and this cycle was repeated in order to monitor spectral changes at pH intervals of approximately 0.1 pH units up to pH 9.0. In order to ensure that the changes were reversible, the pH of the solution was then sequentially lowered and spectra were recorded. Spectra of reacidified solutions were scanned to ensure that they matched those of the starting solutions.

Potentiometric Titrations. In order to determine how many protons were lost as solutions of the rhodium complexes become more basic, known amounts of base were added to aqueous solutions of metal complex and the pH was monitored. Solutions at least 500 μM in metal complex in a known volume of 0.001N HCl (4–5 mL) were stirred in polyethylene beakers fitted with a pH electrode. The solutions were titrated with NaOH (0.001–1.0N) added in 20-μL aliquots. Blank solutions of 0.001N HCl were titrated with base to determine the amount of OH^- consumed by contaminants and dissolved CO_2 from the air, a quantity that was negligible in comparison to that consumed by metal complex.

Ferrioxalate Actinometry. Ferrioxalate actinometry was used to calibrate the photon flux from the Hg/Xe lamp.[17] Photon flux was calibrated before every photolysis experiment, by using six trials and a control at each irradiation wavelength. With our irradiation geometry, the photon flux values for the experiments described fell within the range of (4.18–4.76) × 10^{-7} einsteins/min at 313 nm and (6.22–6.59) × 10^{-7} einsteins/min at 365 nm.

Photolysis of Rhodium(III) Complexes. Solutions of Rh(phen)$_2$(phi)$^{3+}$ and Rh(phi)$_2$(bpy)$^{3+}$ (2 mL, 15 μM) in 25 mM sodium cacodylate, pH 7.5, were added to quartz cuvettes containing a small stir bar. The cuvette was positioned in the focal point of the Hg/Xe lamp and irradiated for time intervals of 1–30 min while the solution was stirred vigorously. The absorbance spectrum of the solution was recorded after each time interval. Care was taken to obtain an array of readings at short time intervals where the reaction was less than 50% complete and the plot of absorbance change versus time was linear. The sample was irradiated and the absorbance spectrum scanned until such time as no further change could be observed in the spectrum. The extent of photoreaction with time was quantitated on the basis of absorbance changes at 368 nm for Rh(phen)$_2$(phi)$^{3+}$ and 350 nm for Rh(phi)$_2$(bpy)$^{3+}$. The photoproduct did not absorb at the monitoring wavelength in the case of Rh(phen)$_2$(phi)$^{3+}$, and for Rh(phi)$_2$(bpy)$^{3+}$, where the photoproduct absorbs slightly, only short time points were considered (where the absorbance of photoproduct was negligible). In the determination of quantum yields for the photoreactions, also only initial irradiation time points were used.

Results

Synthetic Methods. Due to the instability of the phi ligand, the synthetic methods used to obtain phi complexes of ruthenium(II) and rhodium(III) differ from those used to prepare complexes of other ligands, such as the polypyridyls. There are two principal routes for attaching the phi ligand to a metal center (Figure 1). The first of these is shown as Scheme I for the synthesis of Ru(phi)$_3^{2+}$. This method involves the generation of the phi ligand in the presence of metal ion, starting with the more stable phi(TMS)$_2$ species.[3,4,14] The second route involves initial ligation of the stable 9,10-diaminophenanthrene ligand to a metal center. This is followed by air oxidation to generate the coordinated phi complex, as described in Scheme II for the synthesis of Rh(phi)$_2$(bpy)$^{3+}$. For some complexes, such as Ru(phi)$_3^{2+}$, both routes successfully lead to complex formation. Some problems were evident when attempts were made to synthesize Rh(phen)$_2$(phi)$^{3+}$ via Schemes I or II, however. It is well-known that complexes such as [Rh(phen)$_2$Cl$_2$]$^+$ do not readily displace coordinated chloride ligands for a third bidentate ligand without long reaction times and the presence of large amounts of hydrazine.[12] Attempts to add phi(TMS)$_2$ (via Scheme I) or DAP (via Scheme II) to complexes such as [Rh(phen)$_2$Cl$_2$]$^+$ resulted in decomposition of the starting materials. Therefore, a third scheme was developed in which [Rh(phen)$_2$Cl$_2$]$^+$ was rendered more reactive by displacement of the chloride ligands with OH_2 ligands.

NMR Spectra. In aprotic solvents, d^6 metal complexes of the phi ligand have distinctive NMR spectra due to imine N–H resonances, which are well separated from other parts of the spectrum. The relatively sharp N–H resonances are observed between 12.5 and 15.0 ppm, making it simple to determine the symmetry and identity of phi complexes by NMR spectroscopy alone. The resonances are seen approximately 1 ppm further downfield for phi complexes of rhodium(III) compared to their ruthenium(II) congeners.

Crystallographic Characterization of [Ru(bpy)$_2$(phi)](BF$_4$)$_2$. The crystal structure of Ru(bpy)$_2$(phi)$^{2+}$ is the first such structure determined by X-ray diffraction of a metal complex containing the phi ligand. An ORTEP drawing of the structure is shown in Figure 2. Atomic coordinates and temperature factors are given in Table II. Bond lengths and angles are given in Tables III and IV, respectively. Thermal parameters and hydrogen atom coordinates are provided as supplementary material.

The crystal structure shows that the bipyridyl ligands of this complex are relatively unperturbed in structure and are similar to those observed in the structure of Ru(bpy)$_3^{2+}$.[18] The planarity and the normal distribution of aromatic bond lengths and angles within the ligand indicate that the structure of phi is as expected. It was possible to locate imine hydrogen atoms of the phi ligand in the electron density map, and a primary imine bond length of 0.990 (28) Å was obtained. Bond angles between nitrogen atoms on the same ligand to ruthenium are relatively uniform. The overall structure of the complex is that of a distorted octahedron, with the bpy ligands pulled away from the phi ligand. The N(3)–Ru–N(5) bond angle between bpy ligands is pinched to 88.6 (1)°. However, the N(1)–Ru–N(5) and N(2)–Ru–N(3) angles, which are between bpy and phi ligands, are wider (98.0 (1) and 97.4 (1)°, respectively). This result is somewhat surprising, since the phi ligand is certainly less sterically hindered about the metal center than is bpy. The distortion in the octahedron, therefore, probably results from electronic rather than steric effects.

As shown in Table III, the observed Ru–N bond lengths to the phi ligand are very short (2.002 (3) and 2.010 (4) Å) in comparison to the Ru–N bonds to the bipyridyl ligands (average length 2.064 Å).[19] This substantial shortening of the Ru–N bond may indicate that there is significantly more back-bonding to the phi ligand than to the polypyridyl ligand.

(17) Calvert, J. G.; Pitts, J. N. *Photochemistry*; John Wiley and Sons: New York, 1967.

(18) Rillema, P. D.; Jones, D. S. *J. Chem. Soc., Chem. Commun.* **1979**, 849.

(19) This effect was evident also in the structure of Ru(bpy)$_2$(bqdi)$^{2+}$.[1]

Scheme I

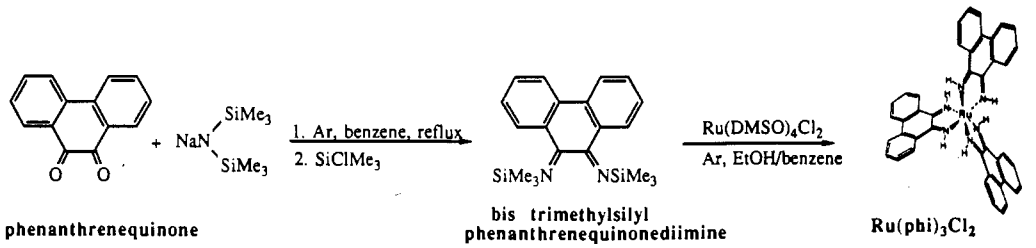

Scheme II

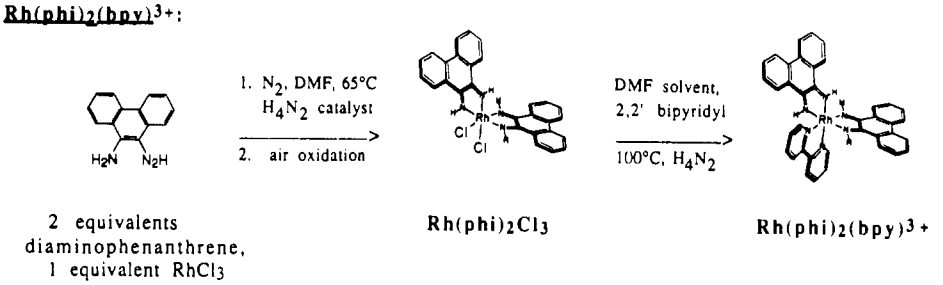

Scheme III

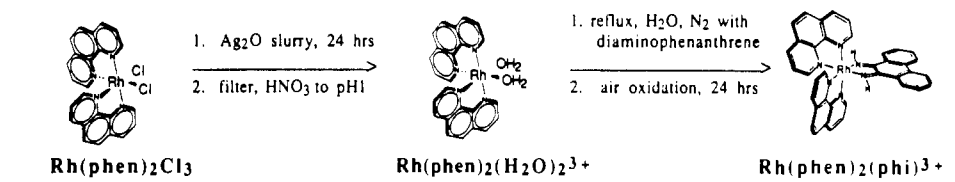

Figure 1. Synthetic strategies to metal complexes containing the phi ligand.

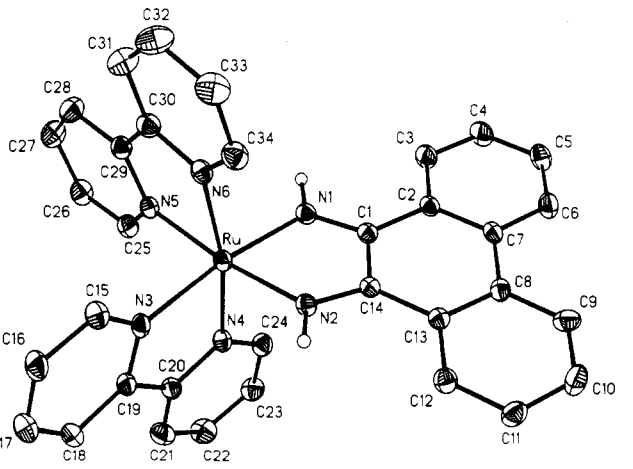

Figure 2. ORTEP diagram of $Ru(bpy)_2(phi)^{2+}$, showing 20% probability thermal ellipsoids. All hydrogen atoms have been omitted except for the imine hydrogen atoms.

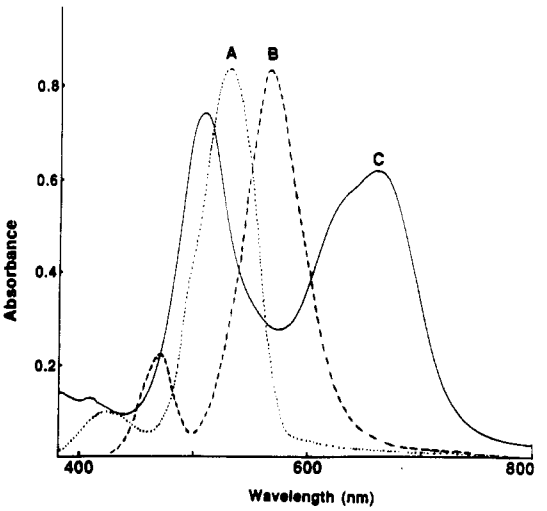

Figure 3. Charge-transfer spectra of mono-, bis-, and trissubstituted complexes of ruthenium containing the phi ligand: (A) $Ru(bpy)_2(phi)^{2+}$ (18 μM); (B) $Ru(phi)_2(bpy)^{2+}$ (17 μM); (C) $Ru(phi)_3^{2+}$ (41 μM). Note the increase in wavelength associated with the charge-transfer band with increasing phi substitution.

Electronic Spectroscopy. Charge-Transfer Spectra of Ruthenium Complexes. The electronic spectra of phi complexes of ruthenium are characterized by unusually intense charge-transfer transitions in the visible region. These transitions, along with the electronic transitions of the rhodium(III) congeners as well as of the ligands, are shown in Table V.

The most outstanding spectroscopic feature of the ruthenium complexes is a progressive red shift in the charge-transfer band over the series $Ru(bpy)_2(phi)^{2+}$, $Ru(phi)_2(bpy)^{2+}$, and $Ru(phi)_3^{2+}$, respectively. This is illustrated in Figure 3. As bpy ligands are replaced by phi ligands in this series of tris(bidentate) chelate ruthenium complexes, the charge-transfer transition moves from 535 nm (in $Ru(bpy)_2(phi)^{2+}$) to 660 nm (in $Ru(phi)_3^{2+}$). This behavior is not seen with other series of mixed-ligand complexes of ruthenium containing MLCT transitions. For example, the charge-transfer transitions for the series $Ru(en)_2(bpy)^{2+}$, $Ru(bpy)_2(en)^{2+}$, and $Ru(bpy)_3^{2+}$ (where en = ethylenediamine) occur

Table II. Atom Coordinates (×10⁴) and Temperature Factors (Å² × 10³) for $[Ru(bpy)_2(phi)](BF_4)_2 \cdot 0.19H_2O$[a]

atom	x	y	z	U_{eq}
Ru	1067 (1)	6933 (1)	6213 (1)	35 (1)*
F(1)	6418 (3)	7232 (2)	4656 (1)	72 (1)*
F(2)	5798 (3)	7322 (2)	5651 (1)	93 (1)*
F(3)	4608 (3)	8049 (2)	4899 (2)	102 (1)*
F(4)	4389 (3)	6674 (2)	4941 (2)	108 (2)*
F(5)	7823 (3)	8196 (2)	7121 (1)	89 (1)*
F(6)	8385 (4)	8555 (2)	8120 (1)	108 (1)*
F(7)	9736 (3)	8970 (2)	7351 (2)	101 (1)*
F(8)	7627 (4)	9511 (2)	7447 (2)	133 (2)*
B(1)	5319 (5)	7327 (3)	5033 (3)	52 (2)*
B(2)	8404 (5)	8810 (3)	7519 (3)	57 (2)*
N(1)	−283 (3)	7879 (2)	6051 (1)	40 (1)*
Hn(1)	−908 (29)	8081 (22)	6373 (12)	46
N(2)	1419 (3)	7303 (2)	5332 (1)	37 (1)*
Hn(2)	2180 (24)	7097 (21)	5078 (13)	44
N(3)	2389 (3)	5904 (2)	6248 (1)	39 (1)*
N(4)	−259 (3)	6002 (2)	5871 (2)	41 (1)*
N(5)	641 (3)	6692 (2)	7142 (1)	38 (1)*
N(6)	2494 (3)	7701 (2)	6692 (2)	40 (1)*
C(1)	−382 (4)	8225 (2)	5492 (2)	37 (1)*
C(2)	−1303 (4)	8914 (2)	5287 (2)	37 (1)*
C(3)	−2214 (4)	9277 (3)	5699 (2)	52 (2)*
C(4)	−3070 (4)	9926 (3)	5502 (2)	58 (2)*
C(5)	−3026 (4)	10223 (3)	4895 (2)	58 (2)*
C(6)	−2142 (4)	9873 (3)	4487 (2)	53 (2)*
C(7)	−1250 (4)	9211 (2)	4670 (2)	38 (1)*
C(8)	−300 (4)	8833 (2)	4223 (2)	41 (1)*
C(9)	−264 (4)	9111 (3)	3600 (2)	55 (2)*
C(10)	601 (5)	8755 (3)	3191 (2)	61 (2)*
C(11)	1462 (4)	8087 (3)	3375 (2)	54 (1)*
C(12)	1476 (4)	7815 (3)	3987 (2)	46 (1)*
C(13)	605 (4)	8174 (2)	4421 (2)	36 (1)*
C(14)	606 (3)	7880 (2)	5066 (2)	33 (1)*
C(15)	3771 (4)	5904 (3)	6423 (2)	51 (2)*
C(16)	4574 (4)	5189 (3)	6434 (2)	57 (2)*
C(17)	3975 (5)	4449 (3)	6248 (2)	64 (2)*
C(18)	2572 (5)	4431 (3)	6065 (2)	55 (2)*
C(19)	1792 (4)	5160 (2)	6078 (2)	42 (1)*
C(20)	278 (4)	5209 (2)	5893 (2)	44 (1)*
C(21)	−577 (5)	4524 (3)	5758 (2)	60 (2)*
C(22)	−1978 (4)	4649 (3)	5588 (2)	64 (2)*
C(23)	−2477 (4)	5441 (3)	5528 (2)	55 (2)*
C(24)	−1606 (4)	6105 (3)	5675 (2)	49 (1)*
C(25)	−326 (4)	6167 (3)	7340 (2)	48 (1)*
C(26)	−502 (4)	6016 (3)	7963 (2)	56 (2)*
C(27)	334 (5)	6432 (3)	8417 (2)	64 (2)*
C(28)	1337 (4)	6972 (3)	8223 (2)	58 (2)*
C(29)	1480 (4)	7094 (2)	7585 (2)	42 (1)*
C(30)	2528 (4)	7654 (3)	7333 (2)	47 (1)*
C(31)	3518 (4)	8092 (3)	7698 (2)	64 (2)*
C(32)	4454 (5)	8601 (3)	7414 (2)	77 (2)*
C(33)	4404 (5)	8650 (3)	6779 (2)	68 (2)*
C(34)	3412 (4)	8199 (3)	6425 (2)	54 (2)*
O_w	6568 (22)	6819 (14)	6755 (10)	103

[a] Asterisk indicates equivalent isotropic U defined as one-third of the trace of the orthogonalized U_{ij} tensor.

Table III. Bond Lengths (Å) of $[Ru(bpy)_2(phi)](BF_4)_2 \cdot 0.19H_2O$

Ru–N(1)	2.002 (3)	Ru–N(2)	2.010 (4)
Ru–N(3)	2.071 (4)	Ru–N(4)	2.055 (3)
Ru–N(5)	2.076 (4)	Ru–N(6)	2.054 (3)
F(1)–B(1)	1.370 (6)	F(2)–B(1)	1.361 (6)
F(3)–B(1)	1.359 (6)	F(4)–B(1)	1.376 (6)
F(5)–B(2)	1.387 (6)	F(6)–B(2)	1.341 (6)
F(7)–B(2)	1.369 (6)	F(8)–B(2)	1.347 (6)
N(1)–Hn(1)	0.990 (28)	N(1)–C(1)	1.307 (5)
N(2)–Hn(2)	0.990 (27)	N(2)–C(14)	1.310 (5)
N(3)–C(15)	1.350 (5)	N(3)–C(19)	1.356 (5)
N(4)–C(20)	1.366 (5)	N(4)–C(24)	1.338 (5)
N(5)–C(25)	1.336 (5)	N(5)–C(29)	1.358 (5)
N(6)–C(30)	1.362 (5)	N(6)–C(34)	1.338 (5)
C(1)–C(2)	1.458 (5)	C(1)–C(14)	1.458 (5)
C(2)–C(3)	1.398 (6)	C(2)–C(7)	1.398 (5)
C(3)–C(4)	1.369 (6)	C(4)–C(5)	1.376 (7)
C(5)–C(6)	1.367 (6)	C(6)–C(7)	1.398 (6)
C(7)–C(8)	1.484 (6)	C(8)–C(9)	1.398 (6)
C(8)–C(13)	1.409 (5)	C(9)–C(10)	1.360 (6)
C(10)–C(11)	1.389 (6)	C(11)–C(12)	1.369 (6)
C(12)–C(13)	1.403 (5)	C(13)–C(14)	1.447 (5)
C(15)–C(16)	1.376 (6)	C(16)–C(17)	1.360 (6)
C(17)–C(18)	1.373 (6)	C(18)–C(19)	1.384 (6)
C(19)–C(20)	1.478 (5)	C(20)–C(21)	1.383 (6)
C(21)–C(22)	1.380 (6)	C(22)–C(23)	1.353 (7)
C(23)–C(24)	1.373 (6)	C(25)–C(26)	1.366 (6)
C(26)–C(27)	1.382 (6)	C(27)–C(28)	1.373 (7)
C(28)–C(29)	1.384 (6)	C(29)–C(30)	1.468 (6)
C(30)–C(31)	1.375 (6)	C(31)–C(32)	1.375 (7)
C(32)–C(33)	1.349 (7)	C(33)–C(34)	1.376 (6)

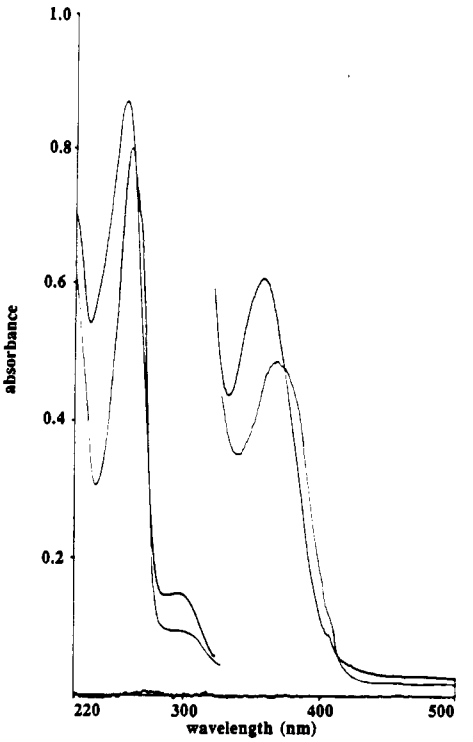

Figure 4. UV–visible spectra of phi$(TMS)_2$ (top scan) and phi (bottom scan). Spectra were recorded in dry heptane and 100:1 heptane/ethanol, respectively. The scale for the plots from 500 to 320 nm is one-tenth that for the spectra recorded from 320 to 220 nm.

at 509, 485, and 456 nm, respectively.[20,21] Not only is there a small difference in λ_{max} over this series, but it is blue-shifted in going from mono- to tris(bipyridyl) derivatives. Clearly, then, there is a striking difference in the nature of the excited state of the phi complexes when compared to other types of ruthenium(II) complexes with N-donor ligands.

Absorption Spectra of Rhodium(III) Complexes. In general, the spectra of phi complexes of rhodium(III) appear to be combinations of the spectra of the component ligands. For example, as can be seen from Table V, the phi-centered $\pi \rightarrow \pi^*$ transition around 360 nm is more intense for $Rh(phi)_2(bpy)^{3+}$ than for $Rh(phen)_2(phi)^{3+}$ because there are more phi ligands on the former complex. Intriguingly, the spectra of $Rh(phen)_2(phi)^{3+}$ and $Rh(phi)_2(phen)^{3+}$ are almost identical.[22] Both are characterized by an intense single band at 272 nm, a shoulder at 300 nm, and an intense absorption at 360 nm. The only noticeable difference is the greater intensity of the phi-centered transition in $Rh(phi)_2(phen)^{3+}$. This phenomenon may be general, as the reported spectra of $Rh(phen)_2(DIP)^{3+}$ and $Rh(DIP)_2(phen)^{3+}$ (where DIP

(20) Kobayashi, H.; Kaizu, Y. *Coord. Chem. Rev.* **1985**, *64*, 53–64.
(21) Brown, G. M.; Weaver, T. R.; Keene, F. R.; Meyer, T. J. *Inorg. Chem.* **1976**, *15*, 190–196.
(22) $Rh(phi)_2(phen)^{3+}$ is synthesized in a manner analogous to that of $Rh(phi)_2(bpy)^{3+}$: Sitlani, A.; Pyle, A. M.; Barton, J. K. Unpublished results.

Table IV. Bond Angles (deg) of $[Ru(bpy)_2phi](BF_4)_2 \cdot 0.19H_2O$

N(1)-Ru-N(2)	76.3 (1)	N(1)-Ru-N(3)	171.8 (1)
N(2)-Ru-N(3)	97.4 (1)	N(1)-Ru-N(4)	96.2 (1)
N(2)-Ru-N(4)	91.2 (1)	N(3)-Ru-N(4)	78.5 (1)
N(1)-Ru-N(5)	98.0 (1)	N(2)-Ru-N(5)	173.5 (1)
N(3)-Ru-N(5)	88.6 (1)	N(4)-Ru-N(5)	92.7 (1)
N(1)-Ru-N(6)	92.0 (1)	N(2)-Ru-N(6)	98.1 (1)
N(3)-Ru-N(4)	94.1 (1)	N(4)-Ru-N(6)	168.8 (1)
N(5)-Ru-N(6)	78.7 (1)	F(1)-B(1)-F(2)	109.8 (4)
F(1)-B(1)-F(3)	111.4 (4)	F(2)-B(1)-F(3)	109.9 (4)
F(1)-B(1)-F(4)	110.2 (4)	F(2)-B(1)-F(4)	107.9 (4)
F(3)-B(1)-F(4)	107.6 (4)	F(5)-B(2)-F(6)	109.7 (4)
F(5)-B(2)-F(7)	108.4 (4)	F(6)-B(2)-F(7)	112.0 (4)
F(5)-B(2)-F(8)	108.7 (4)	F(6)-B(2)-F(8)	108.7 (5)
F(7)-B(2)-F(8)	109.3 (4)	Ru-N(1)-H_n(1)	122.6 (18)
Ru-N(1)-C(1)	118.9 (3)	H_n(1)-N(1)-C(1)	118.5 (17)
Ru-N(2)-H_n(2)	125.6 (17)	Ru-N(2)-C(14)	118.6 (2)
H_n(2)-N(2)-C(14)	115.8 (17)	Ru-N(3)-C(15)	126.4 (3)
Ru-N(3)-C(19)	116.1 (2)	C(15)-N(3)-C(19)	117.5 (3)
Ru-N(4)-C(20)	115.9 (2)	Ru-N(4)-C(24)	125.5 (3)
C(20)-N(4)-C(24)	118.4 (3)	Ru-N(5)-C(25)	126.7 (3)
Ru-N(5)-C(29)	115.3 (2)	C(25)-N(5)-C(29)	117.9 (3)
Ru-N(6)-C(30)	115.8 (2)	Ru-N(6)-C(34)	125.2 (3)
C(30)-N(6)-C(34)	118.9 (3)	N(1)-C(1)-C(2)	126.7 (3)
N(1)-C(1)-C(14)	113.1 (3)	C(2)-C(1)-C(14)	120.1 (3)
C(1)-C(2)-C(3)	120.9 (4)	C(1)-C(2)-C(7)	118.6 (3)
C(3)-C(2)-C(7)	120.5 (3)	C(2)-C(3)-C(4)	120.4 (4)
C(3)-C(4)-C(5)	119.5 (4)	C(4)-C(5)-C(6)	120.7 (4)
C(5)-C(6)-C(7)	121.5 (4)	C(2)-C(7)-C(6)	117.4 (4)
C(2)-C(7)-C(8)	121.5 (3)	C(6)-C(7)-C(8)	121.2 (4)
C(7)-C(8)-C(9)	122.0 (3)	C(7)-C(8)-C(13)	120.1 (3)
C(9)-C(8)-C(13)	117.9 (4)	C(8)-C(9)-C(10)	121.6 (4)
C(9)-C(10)-C(11)	121.0 (4)	C(10)-C(11)-C(12)	118.7 (4)
C(11)-C(12)-C(13)	121.6 (4)	C(8)-C(13)-C(12)	119.2 (3)
C(8)-C(13)-C(14)	119.2 (3)	C(12)-C(13)-C(14)	121.7 (3)
N(2)-C(14)-C(1)	112.8 (3)	N(2)-C(14)-C(13)	126.9 (3)
C(1)-C(14)-C(13)	120.3 (3)	N(3)-C(15)-C(16)	122.6 (4)
C(15)-C(16)-C(17)	119.5 (4)	C(16)-C(17)-C(18)	119.1 (4)
C(17)-C(18)-C(19)	119.7 (4)	N(3)-C(19)-C(18)	121.6 (3)
N(3)-C(19)-C(20)	114.4 (3)	C(18)-C(19)-C(20)	124.0 (4)
N(4)-C(20)-C(19)	114.6 (3)	N(4)-C(20)-C(21)	120.6 (4)
C(19)-C(20)-C(21)	124.7 (4)	C(20)-C(21)-C(22)	119.4 (4)
C(21)-C(22)-C(23)	119.4 (4)	C(22)-C(23)-C(24)	119.7 (4)
N(4)-C(24)-C(23)	122.3 (4)	N(5)-C(25)-C(26)	123.3 (4)
C(25)-C(26)-C(27)	119.3 (4)	C(26)-C(27)-C(28)	118.4 (4)
C(27)-C(28)-C(29)	119.8 (4)	N(5)-C(29)-C(28)	121.4 (4)
C(5)-C(29)-C(30)	115.0 (3)	C(28)-C(29)-C(30)	123.6 (4)
N(6)-C(30)-C(29)	115.1 (3)	N(6)-C(30)-C(31)	120.4 (4)
C(29)-C(30)-C(31)	124.5 (4)	C(30)-C(31)-C(32)	119.9 (4)
C(31)-C(32)-C(33)	119.3 (5)	C(32)-C(33)-C(34)	119.8 (5)
N(6)-C(34)-C(33)	121.7 (4)		

= 4,7-diphenylphenanthroline) are also differential linear combinations of spectra from DIP and phenanthroline ligands.[23,24]

Phi and Phi(TMS)$_2$. The absorbance spectra of Rh(III) complexes cannot be interpreted in the absence of an understanding of their component ligands. The spectra of phi and phi(TMS)$_2$ are shown in Figure 4. The most distinguishing feature of both phi and the protected phi ligand is the intense $\pi \rightarrow \pi^*$ transition at 360 and 368 nm, respectively. The presence of a coordinated metal (or the presence of a silyl group) on the nitrogen atoms tends to modulate the wavelength of this phi ligand-centered transition.

Nonemissive Character of Ruthenium and Rhodium Complexes. Emission and excited-state absorption spectroscopy were performed on $Ru(bpy)_2(phi)^{2+}$ and $Ru(phi)_3^{2+}$. Although experiments were conducted in the presence and absence of oxygen, at room temperature and at 77 K, no emission could be detected from these complexes. Importantly, excited-state absorption experiments indicate the excited-state lifetime to be shorter than 6 ns (the lifetime of the pulse).[4] Attempts to detect luminescence at room temperature from $Rh(phen)_2(phi)^{3+}$ and $Rh(phi)_2(bpy)^{3+}$ also failed, although work is presently underway to examine luminescence from these complexes at 77 K.[25]

Table V. UV-Visible Spectra of Phi Complexes of Ruthenium(II) and Rhodium(III)

complex	electronic transitions λ_{max}, nm ($10^{-3}\epsilon$, M^{-1} cm^{-1})
$Ru(phen)_2(phi)^{2+}$	535 (51.9) (CT), 416 (broad, 13.3), 380 (broad, 12.9), 290 (s, 51.5), 262 (151.1)
$Ru(bpy)_2(phi)^{2+}$	535 (48.0) (CT), 427 (10.2) (CT), 284 (87.8), 266 (61.3), 252 (68.3), 244 (s, 60.5)
$Ru(phi)_2(bpy)^{2+}$	572 (75.3) (CT), 473 (31.0) (CT), 280 (s, 91.3), 254 (108.8)
$Ru(phi)_3^{2+}$	660 (15.2) (CT), 640 (13.6) (CT), 510 (18.2) (CT), 380 (4.0), 300 (22.5), 256 (45.0)
$Rh(phen)_2(phi)^{3+}$	358 (19.4), 300 (s, 34.0), 272 (116.2)[a]
$Rh(phi)_2(bpy)^{3+}$	378 (28.2), 312 (s, 30.0), 292 (43.2), 270 (64.2), 262 (s, 62.4), 250 (s, 67.4)[b]
$Rh(phi)_3^{3+}$	408 (9.9), 350 (10.0)[c]
phi	368, 296 (s), 262
phi(TMS)$_2$	360, 296, 258
bpy	281, 243, 235
phen	264, 230, 226 (s)

[a] Measured in pH 7 tris-acetate buffer. pH-independent isosbestic points on the spectrum occur at 362 nm (ϵ = 19 400 M^{-1} cm^{-1}), and 318 (17 200 M^{-1} cm^{-1}). Concentrations were measured only at these constant wavelengths. Throughout the table, s = shoulder. [b] Measured in pH 7 tris-acetate buffer. pH-independent isosbestic point occurs at 350 nm (ϵ = 23 600 M^{-1} cm^{-1}). Solution concentration measured only at this constant wavelength. [c] Extinction coefficient determined by weighing solid. Spectrum measured in H_2O, in which the complex is only sparingly soluble.

Acid-Base Properties of Phi Complexes. Rhodium Complexes. The absorption spectra of phi complexes of rhodium(III) change dramatically depending on the pH of the solution. As the pH of a $Rh(phen)_2(phi)^{3+}$ solution is titrated from 4.5 to 9.0, one observes a blue shift of 20 nm in the maximum wavelength of the phi-centered transition (centered at 356 nm at pH 7.0). Although transitions below 350 nm are sensitive to the pH as well, the most substantial perturbation is evident in this peak, which, in addition to shifting, shows a 12% drop in overall intensity over the pH range studied (Figure 5). Isosbestic points are observed at 362 and 318 nm. These spectroscopic changes with pH are completely reversible; reacidification of pH 9 solutions yields spectra identical with those obtained initially at low pH. A plot of the phi absorption maximum versus pH yields a curve with an inflection point at pH 6.2.

Direct potentiometric titrations were performed in order to correlate the spectroscopic results with the acid-base properties of the complex. The potentiometric titration yielded a plot with an inflection point at pH 6.0, paralleling the spectroscopic results, with a corresponding consumption of 1.3 protons. Importantly, no evidence of precipitation was observed with $Rh(phen)_2(phi)^{3+}$ at high pH.

Even more dramatic pH-dependent spectral shifts are seen with $Rh(phi)_2(bpy)^{3+}$, and as observed with $Rh(phen)_2(phi)^{3+}$, they are completely reversible. In this case, the phi-centered transition shifts 29.7 nm to the blue when titrated from pH 4.0 to 9.2 (Figure 5B). The primary isosbestic point is found at 350 nm. A plot of the wavelength maximum of the phi-centered transition versus pH yields a pH titration curve with an inflection point at pH 6.9. The intensity of the transition is affected even more substantially than that of $Rh(phen)_2(phi)^{3+}$, decreasing by 34%. Potentiometric titration of concentrated $Rh(phi)_2(bpy)^{3+}$ solutions with base yielded broader titration curves with inflection points at approximately pH 6.8. The quantitation corresponds to the loss of two protons upon basification to pH 9.0. Both optical and potentiometric methods are in agreement and indicate that the pK_a's of $Rh(phi)_2(bpy)^{3+}$ occur at approximately pH 6.8–6.9. Again, no evidence of precipitation at high pH was observed. Results of these studies are summarized in Table VI.

Ruthenium Complexes. Optical pH titrations on the ruthenium(II) analogues, notably $Ru(phen)_2(phi)^{3+}$, showed no change in the maximum wavelength of the charge-transfer band with

(23) Rehmann, J. P. Ph.D. Thesis, Columbia University, 1988.
(24) Kirshenbaum, M. R. Ph.D. Thesis, Columbia University, 1989.
(25) Friedman, A.; Barton, J. K. Unpublished results.

Table VI. pH Dependence of Phi Complexes of Rhodium(III) and Their Spectra

complex	blue shift in λ_{max},[a] nm	intensity change,[b] %	isosbestic points, nm (ϵ)[c]	pK_a optical[d]	pK_a direct[e]	no. of protons lost[f]
$Rh(phen)_2(phi)^{3+}$	20.1	12.2	362 (19400) 318 (17200)	6.2	6.0	1.3
$Rh(phi)_2(bpy)^{3+}$	29.7	34.0	350 (23600)	6.9	6.8	2.0

[a] The extent of shift in the low-energy phi-centered transition when the pH is raised from 4.0 to 9.0. [b] The decrease in intensity of the phi transition at pH 9.0 with respect to its intial intensity at pH 4.0. [c] Points on the spectra insensitive to pH changes, listed with ϵ values (M^{-1} cm^{-1}). Ideal wavelengths for concentration determination. [d] Determined as the inflection point of a plot of phi transition λ_{max} vs pH. [e] Determined as the inflection point of a plot of moles of OH^- consumed by the Rh complex vs pH. [f] Equivalents of OH^- required for saturation (the plateau of a plot described in footnote *e*). This represents the number of protons lost by a given metal complex.

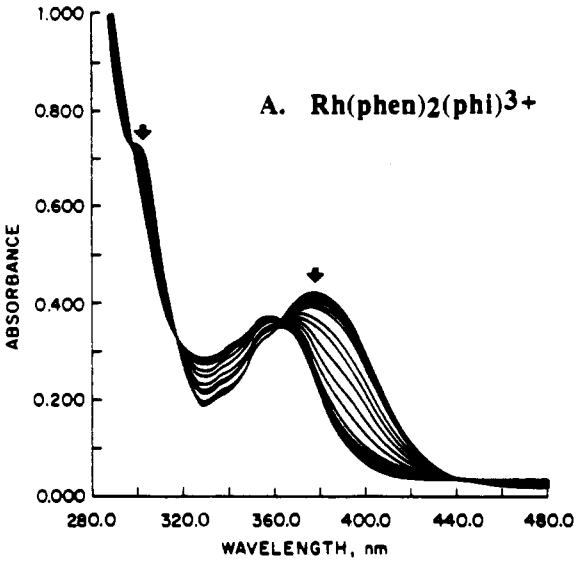

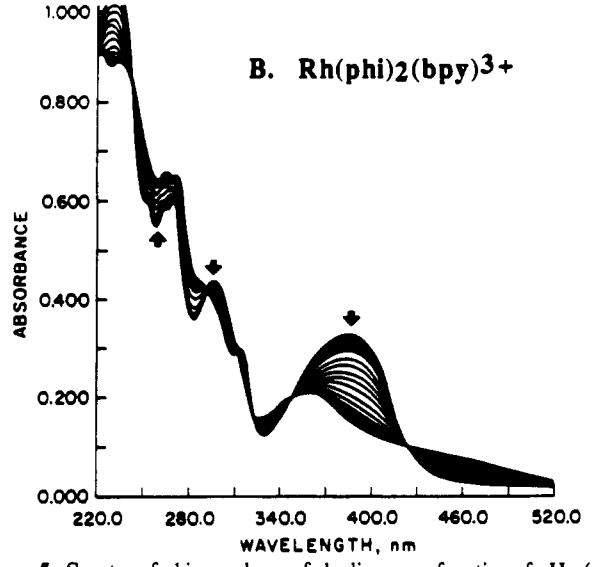

Figure 5. Spectra of phi complexes of rhodium as a function of pH: (A) $Rh(phen)_2(phi)^{3+}$; (B) $Rh(phi)_2(bpy)^{3+}$. Arrows indicate the starting spectra at pH 4.

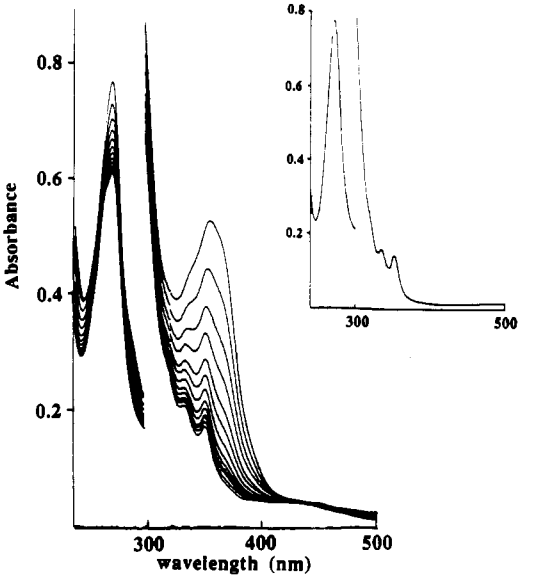

Figure 6. Photolysis of $Rh(phen)_2(phi)^{3+}$ monitored by UV–visible spectroscopy. Irradiation of the complex leads to the production of $[Rh(phen)_2(OH_2)_2]^{3+}$. The spectrum of authentic $[Rh(phen)_2(OH_2)_2]^{3+}$, obtained synthetically, is shown as the inset for comparison. Note the correspondence between the photoproduct (final scan) and the absorbance maxima at 334 and 352 nm for $[Rh(phen)_2(OH_2)_2]^{3+}$. The solution containing $Rh(phen)_2(phi)^{3+}$ (13.4 μM) was scanned after every 10 min of irradiation at 313 nm. The scale for the plots from 500 to 320 nm is one-fourth that for the spectra recorded from 320 to 220 nm.

increasing pH (from 2 to 11). No spectroscopic changes of any kind as a function of pH were noted. The spectrum of $Ru(phi)_3^{2+}$ is nonetheless highly solvent dependent.[4] Controlled quantitative potentiometric studies with $Ru(phi)_2(bpy)^{2+}$ were not possible owing to problems of solubility.

Photoreactivity of Rh(III) Phi Complexes. Upon irradiation at 313 or 365 nm, phi complexes of rhodium(III) undergo decomposition. As shown in Figure 6, $Rh(phen)_2(phi)^{3+}$ shows a dramatic decrease in the intensity of its phi-centered transition at 360 nm. After irradiation for 2 h, the phi transition is completely eliminated and the final spectrum appears identical with that of bis(phenanthroline) derivatives of rhodium(III), $[Rh(phen)_2Cl_2]^+$ or $[Rh(phen)_2(H_2O)]^{3+}$ (inset, Figure 6). This indicates strongly that photolysis results in a photodecomposition pathway involving dissociation of the phi ligand, leaving the spectroscopically stable $Rh(phen)_2^{3+}$ moiety.

Irradiation of $Rh(phi)_2(bpy)^{3+}$ also results in substantial decreases in the intensity of the phi-centered transition at 356 nm, indicating that the phi ligand is involved in photodecomposition in this case as well. However, continuous irradiation does not result in an identifiable photoproduct. The spectrum ceases to change with further irradiation at 313 nm after 24 h, and the absorption of the photoproduct resembles that of phi complexes at 356 nm. This is not surprising given that the loss of one phi ligand would produce first a species such as $[Rh(bpy)(phi)(OH_2)_2]^{3+}$. The final photoproduct absorbs with approximately 36% of the intensity at 356 nm as the parent $Rh(phi)_2(bpy)^{3+}$.

Plots of photodecomposition versus reaction time were linear, allowing the determination of quantum yields for the photodissociation. The quantum yield data are summarized in Table VII. These data indicate the photodissociation of $Rh(phen)_2(phi)^{3+}$ to be 3 times more efficient at 313 nm than at 365 nm. Photodissociation yields for $Rh(phi)_2(bpy)^{3+}$ at 365 nm was too low to measure quantitatively. Nonetheless, at 313 nm the photodissociation of $Rh(phen)_2(phi)^{3+}$ is 13 times more efficient than that of $Rh(phi)_2(bpy)^{3+}$. This result is particularly important in interpreting the differences in DNA photocleavage efficiency with the two molecules.

Discussion

Synthesis and Structure of Phi Complexes. Mixed-ligand complexes of ruthenium(II) and rhodium(III) that contain the

Table VII. Photochemical Parameters for Phi Complexes of Rhodium(III)

complex	irradiation wavelength, nm	k_{rel} (photodecomposn),[a] min^{-1}	quantum yield for photodecomposn[b] (std dev)
$Rh(phen)_2(phi)^{3+}$	313	1.1×10^{-2} ($R = 0.996$)	$2.7\ (3) \times 10^{-3}$
	365	3.4×10^{-3} ($R = 0.991$)	$6.2\ (5) \times 10^{-4}$
$Rh(phi)_2(bpy)^{3+}$ [c]	313	8.3×10^{-4} ($R = 0.997$)	$2.1\ (4) \times 10^{-4}$

[a] Defined as the slope of a linear plot of the concentration of rhodium complex reacted divided by the initial rhodium concentration versus time of irradiation. [b] Moles of photoproduct $[Rh(phen)_2(H_2O)_2^{3+}]$ formed per unit time per moles for photons absorbed per unit time. [c] The photoreaction of $Rh(phi)_2(bpy)^{3+}$ at 365 nm was found to be too slow too allow reliable quantitation.

phi ligand may be prepared through a variety of strategies. Owing to the instability of the phi ligand in solution, direct ligand coordination may be accomplished only via addition of silylated phi to the metal ion in an inert atmosphere. The alternate strategies involve coordination first of the stable diaminophenanthrene to the metal center followed by an intramolecular redox reaction to obtain the oxidized, coordinated phi complex. Despite the instability of the phi ligand, then, substantial synthetic flexibility is still available.

The crystal structure of $Ru(bpy)_2(phi)^{2+}$ shows the expansive, aromatic structure that may be considered as characteristic of the phi ligand. The bond lengths and angles are completely consistent with the phi ligand as a coordinated *o*-diimine moiety. Substantial back-bonding between the phi and metal center is evident, far more so than is found with polypyridyl ligands. The phi nitrogen atoms are pulled closely into the metal center. Owing to the substantial electronic interaction of the phi ligand with the metal center, the remaining ligands are pinched back (decreasing the angle between coordinated bpy ligands), causing phi to extend far out from the center of the complex. This novel shape of the coordinated ligand, jutting out from the metal center, has been extremely advantageous in the design of DNA-binding molecules. These indications of substantial back-bonding to the phi ligand also support previous quantum mechanical studies which suggested that the phi ligand should have an unusually large π-acceptor capability.[26]

Novel Electronic Characteristics of Phi Complexes of Ruthenium(II). The increased π-acceptor ability of the phi ligand in comparison to polypyridyls is evident also in the charge-transfer spectra of the ruthenium complexes. The MLCT bands are shifted to lower energies for ruthenium complexes containing phi. More surprising, however, is the apparent delocalized character to these charge-transfer states in comparison to the localized charge transfers apparent more commonly. Much evidence supports the notion that the MLCT transition in ruthenium(II) polypyridyls is localized onto each ligand, rather than being considered as delocalized over the full liganded framework. In particular, excited-state resonance Raman spectroscopic studies[27] indicate that $Ru(bpy)_3^{2+*}$ displays a spectrum consistent with that of $[Ru(III)(bpy)_2(bpy^-)]^{2+}$. As a result of this localized character, the MLCT transitions of ruthenium(II) polypyridyls do not red shift with increasing polypyridyl substitution. In general, there are only small differences in the electronic spectra within a series of mono-, bis-, and tris(bipyridyl)-substituted ruthenium(II) complexes where other ligands are N-donors. The sharp contrast found with ruthenium complexes containing increasing phi substitution indicates that the electronic character of the phi complexes must be fundamentally different from those of the polypyridyl complexes. Indeed the intense transitions found in the phi complexes may instead represent an example of a completely delocalized charge transfer. This notion is suggested by the observation of dramatic red-shifting in the MLCT states with increasing phi substitution. Just as we observe that delocalization of π electrons over more nuclei results in lower energy π–π^* transitions, increasing the number of phi ligands around the metal would lower the energy of the MLCT transition through delocalization over all three ligands.

This notion cannot, however, be tested through excited-state resonance Raman spectroscopy. In the phi complexes, the excited-state lifetime is too short for practical measurements to be obtained.[4] Also owing to the short excited-state lifetime of the complexes and in contrast to the case for ruthenium(II) polypyridyls, no luminescence is observed. Perhaps these features are linked also to a delocalized character in the MLCT transition.

A number of applications for phi complexes of ruthenium(II) are already evident, despite the absence of luminescence. The complexes bind avidly to DNA[5,6,9,11] and may serve as excellent markers for electron microscopy or scanning tunneling microscopy. It appears that the MLCT transition of $Ru(phi)_2(bpy)^{2+}$ is among the most intense observed for a mononuclear Ru(II) complex. With an extinction coefficient of 73 500 M^{-1} cm^{-1} at 572 nm, this complex has an intense blue color that is visible at micromolar levels. The MLCT charge transfer in $Ru(phi)_3^{2+}$, furthermore, at 660 nm appears to be the lowest energy transition observed for a mononuclear ruthenium(II) complex.[28] These complexes may therefore show promise as novel stains for various biological imaging processes.

pH Sensitivity of Rh(III) Phi Complexes. The substantial π acidity of the phi ligand is evident also in the rhodium complexes. Rh(III) phi complexes undergo reversible deprotonations in the physiological pH range. The complexes are stable over a broad pH range, but dramatic perturbations are evident in both wavelength and intensity of their phi-centered electronic transitions as a function of pH. Differences between $Rh(phen)_2(phi)^{3+}$ and $Rh(phi)_2(bpy)^{3+}$ pH effects appear to be due largely to the stoichiometry of phi substitution, indicating that the ligands behave independently of one another, in proportion to their numbers. At pH 8, the complexes may be more properly represented as $Rh(phen)_2(phi)^{2+}$ and $Rh(phi)_2(bpy)^{+}$. The fact that the rhodium(III) complexes are so sensitive to pH while the ruthenium(II) analogues are not is likely the result of the more electropositive nature of the rhodium(III) center. The color change on deprotonation might be explained by a charge localization onto the exocyclic imines in the excited state, a process that would be disfavored with deprotonation, leading to the observed blue shift.

Photochemistry of Phi Complexes. The phi complexes of rhodium not only bind to DNA avidly but also upon photoactivation promote strand scission.[6,9,11] It is therefore important to begin to characterize the photoreactions of these complexes not only in the presence but also in the absence of DNA. Phi complexes of ruthenium(II), in contrast, appear to be photostable and do not promote DNA cleavage in the presence of light.

Both $Rh(phen)_2(phi)^{3+}$ and $Rh(phi)_2(bpy)^{3+}$ complexes appear to undergo photodecomposition upon irradiation at 313 and 365 nm with dissociation of the phi ligand.

$$RhL_2(phi)^{3+} \xrightarrow{h\nu} RhL_2(OH_2)_2^{3+} + \text{phi decomposition product}$$

where L is a bidentate N-donor ligand. UV–visible spectroscopy as a function of irradiation of $Rh(phen)_2(phi)^{3+}$ indicates the clean formation of the $Rh(phen)_2(OH_2)_2^{3+}$ species. Because of the instability of the dissociated phi complex, further decomposition

(26) Reinhold, J.; Benedix, R.; Birner, P.; Hennig, H. *Inorg. Chim. Acta* **1979**, *33*, 209–213.

(27) Caspar, J. V.; Westmoreland, T. D.; Allen, G. H.; Bradley, P. G.; Meyer, T. J.; Woodruff, W. H. *J. Am. Chem. Soc.* **1984**, *106*, 3492–3500. Bradley, P. G.; Kress, N.; Hornberger, B. A.; Dallinger, R. F.; Woodruff, W. H. *J. Am. Chem. Soc.* **1981**, *103*, 7441–7446. Dallinger, R. F.; Woodruff, W. H. *J. Am. Chem. Soc.* **1979**, *101*, 4391–4393.

(28) Blue ruthenium species have been reported previously, but while their structures remain elusive, they have been formulated as multinuclear species: Rose, D.; Wilkinson, G. *J. Chem. Soc. A* **1970**, 1791.

of the ligand ensues. DNA photocleavage experiments also indicate that the rhodium complexes promote photooxidation of DNA through direct H-atom abstraction.[6,29] The experiments described here cannot in fact distinguish between a simple photoanation and photoreduction of the metal complex followed by air oxidation back to the Rh(III) state (especially given the decomposition of the resultant dissociated phi ligand), but on the basis of comparisons to $Rh(phen)_3^{2+}$, which can serve as a powerful photooxidant,[30] such a route is likely. Here, however, we consider only the net reaction, that of photoanation.

There are many parallels evident in the photoreactions of the phi and polypyridyl complexes of rhodium(III). Irradiation of $Rh(bpy)_3^{3+}$ leads to the production of $[Rh(bpy)_2(H_2O)_2]^{3+}$ and free bpy ligand in a reaction that closely resembles the photolysis of $Rh(phen)_2(phi)^{3+}$.[31,32] Also comparable are the quantum yields for photodissociation. The quantum yields determined for $Rh(phen)_2(phi)^{3+}$ and $Rh(phi)_2(bpy)^{3+}$ photoaquation at 313 nm are 2.7×10^{-3} and 0.2×10^{-3}, respectively. These values are very close to the quantum yield of photoaquation for $Rh(bpy)_3^{3+}$, which has a value of 2.4×10^{-3}.[33] Furthermore, the quantum yields for the photoaquation of $Rh(DIP)_3^{3+}$, $Rh(phen)_3^{3+}$, $Rh(phen)_2(DIP)^{3+}$, and $Rh(DIP)_2(phen)^{3+}$ have been shown to be 1.0×10^{-3}, 1.4×10^{-3}, 0.5×10^{-3}, and 0.22×10^{-3}, respectively.[34,35] Therefore, the quantum yields for photodissociation of a wide variety of tris-substituted and mixed-ligand complexes of rhodium(III) are quite close one to another, further suggesting that the initial photoreaction of phi complexes is similar in nature to that of the well-studied rhodium(III) polypyridyls. Interestingly, in the case of the mixed-ligand phi systems, it is phi dissociation that is first evident, not phenanthroline or a mixture of both. Thus, in the mixed-ligand series, the primary photoreaction is phi centered, leading to its preferential labilization.

The similarities in the photoreaction products and in the quantum yields of photoaquation suggest then that the excited state of the phi complexes may resemble that of the rhodium(III) polypyridyls. The excited state of the polypyridyl analogues is considered to be a ligand-centered $\pi \rightarrow \pi^*$ triplet state that undergoes rapid intersystem crossing to a metal-centered d–d state.[30] The ability of these complexes to function as powerful photooxidants[36] lies in the nature of this ligand-centered triplet and in the nature of the $[Rh^{II}(bpy)_2(bpy^{\bullet+})]^{3+}$ state that results from it.[37]

Conclusion

The development of relatively simple preparations for phi complexes of ruthenium(II) and rhodium(III) has lead to a new family of coordination complexes with unique structural, physical, and photophysical properties. The phi ligand shows substantial π-back-bonding interactions with the metal center and provides an expansive aromatic ligand jutting out from the metal, which can be exploited in various probe designs. The ruthenium analogues provide new evidence for the existence of an unusual delocalized charge-transfer state. The photochemically reactive rhodium analogues have already demonstrated their utility as biological structure probes and appear to share the photochemistry of their polypyridyl counterparts. Given the rapidity with which uses for these new complexes have been found, transition-metal complexes that incorporate the phi ligand should represent promising inorganic materials for future applications.

Acknowledgment. We are grateful to the National Institutes of Health (Grant GM33309) for their financial support.

Supplementary Material Available: Full listings of anisotropic temperature factors (Table SI) and hydrogen atom coordinates and temperature factors (Table SII) (3 pages); a complete table of structure factors (Table SIII) (19 pages). Ordering information is given on any current masthead page.

(29) Besides demonstrating H-atom abstraction, experiments with DNA indicate the formation of phenanthrenequinone and a dimeric condensation product of phenanthrenequinone and phi upon decomposition of the dissociated phi. The parallel decomposition likely occurs in the absence of DNA and is evident spectroscopically in the 400–500-nm region of the spectrum shown in Figure 6. Long, E. C.; Absalon, M.; Stubbe, J.; Barton, J. K., submitted for publication.

(30) Indelli, M. T.; Carioli, A.; Scandola, F. *J. Phys. Chem.* **1984**, *88*, 2685–2686. Ballardini, R.; Varani, G.; Balzani, V. *J. Am. Chem. Soc.* **1980**, *102*, 1719.
(31) Chan, S.-F.; Chou, M.; Creutz, C.; Matsubara, T.; Sutin, N. *J. Am. Chem. Soc.* **1981**, *103*, 369–379.
(32) Brown, G. M.; Chan, S.-F.; Creutz, C.; Schwartz, H. A.; Sutin, N. *J. Am. Chem. Soc.* **1979**, *101*, 7639–7640.
(33) Vogler, A.; Kunkely, H. *Inorg. Chem.* **1987**, *26*, 1819–1820.
(34) Rund, J. V. *Inorg. Chem.* **1968**, *7*, 24. Kulasingam, G. C.; McWhinnie, W. R.; Miller, J. D. *J. Chem. Soc. A* **1969**, 521–524.
(35) Saliby, M. J.; Kaplan, E. B.; Sheridan, P. S.; Madan, S. K. *Inorg. Chem.* **1981**, *20*, 728–733. Lay, P. A.; Sargeson, A. M. *Inorg. Synth.* **1986**, *24*, 283–287.
(36) Frink, M. E.; Sprouse, S. D.; Goodwin, H. A.; Watts, R. J.; Ford, P. C. *Inorg. Chem.* **1988**, *27*, 1283–1286.
(37) This model involving metal photoreduction can also nicely account for the DNA photocleavage results.[6,29]